Applied Surface Science 629 (2023) 157333

Contents lists available at ScienceDirect

Applied Surface Science

journal homepage: www.elsevier.com/locate/apsusc

Full Length Article

Immobilized di(hydroperoxy)propane adducts of phosphine oxides as traceless and recyclable oxidizing agents

John C. Hoefler, Anh Vu, Arturo J. Perez, Janet Blümel *

Department of Chemistry, Texas A&M University, College Station, TX 77845-3012, United States

A B S T R A C T

Oxidations represent important reactions that are ubiquitous in academia and industry. Hydrogen peroxide (H_2O_2) is a common source of active oxygen for oxidations. H_2O_2 is usually diluted in water as it is too unstable to be used in pure form. However, the presence of water can complicate reactions because biphasic mixtures with organic solvents form. Furthermore, secondary reactions with water may lead to side products. Therefore, alternative forms of H_2O_2, such as peroxide adducts, are an active area of research. Di(hydroperoxy)alkane adducts of phosphine oxides are one attractive solution because they are soluble in organic solvents, crystallizable, shelf-stable and active towards a variety of oxidation reactions. The only drawback is that the phosphine oxide carrier has to be removed after the reaction. In this contribution, the bifunctional ligand $(EtO)_3Si(CH_2)_2PPh_2$ is immobilized on a silica (SiO_2) support which is subsequently end-capped with $EtOSi(CH_3)_3$. The new surface-bound di(hydroperoxy)propane adduct is then generated with the immobilized phosphine oxide as carrier. The adduct and a deuterated analog are characterized with solid-state and solution NMR spectroscopy. It has been demonstrated that substrates in organic solvents easily access the surface-bound peroxide and are oxidized quantitatively. The phosphine oxide carrier remains bound to the surface and can be removed easily by settling of the silica. Using the oxidative esterification of nonyl aldehyde it is proven that the immobilized peroxide adduct does not leach from the silica support and is active and reusable over multiple cycles.

1. Introduction

Hydrogen peroxide (H_2O_2) is a ubiquitous oxidant in industry and academia due to its applicability to a diverse array of oxidation reactions [1–3]. The H_2O_2 market, already a multi-billion-dollar industry, is only expected to grow over the coming years due to increased demand from various industrial sectors [4]. Despite its widespread use, a significant drawback of H_2O_2 is the need to dilute it in aqueous solution. Many common organic solvents are immiscible with water. This limits the solvent choice and most often necessitates biphasic reactions to be performed which slows the reaction rates and complicates work-up procedures. Water can also lead to secondary reactions and the formation of undesired side-products that reduce the product yield and necessitate further purification. Finally, aqueous H_2O_2 decays at an unpredictable rate, necessitating titrations if a stoichiometric amount is required [5].

To circumvent these issues while still maintaining the impressive reactivity of H_2O_2, solid forms of peroxides are an active area of research. Since phosphine oxides readily engage with different HO groups via strong hydrogen bonds [6–10], they can be used to stabilize hydrogen peroxide and di(hydroperoxy)alkanes to form Hilliard [11–13] and Ahn [13–18] adducts, respectively. All phosphine oxide adducts are attractive options as solid peroxides because they are robust and long-lived, their composition is well-defined on the molecular level, and they are soluble in organic solvents [11–18]. Ahn adducts in particular are thermally and mechanically stable, and they crystallize readily, allowing for easy purification and characterization by single crystal X-ray diffraction [13–18]. Ahn adducts are easily formed by combining the phosphine oxide with hydrogen peroxide and a ketone. For example, to synthesize the specific adduct $Ph_3PO{\bullet}(HOO)_2CMe_2$, acetone is used as the ketone in combination with Ph_3PO as the carrier [13]. Ahn adducts have been successfully employed in a variety of reactions such as selective phosphine oxidation [13,14,16], sulfide to sulfoxide oxidation [13], the direct oxidative esterification of aldehydes [18], and Baeyer-Villiger oxidations of cyclic ketones.[17] Due to the high solubility of the Ahn adducts, these reactions can be performed in one organic phase and without the need for an additional oxygen transfer mediator. This renders di(hydroperoxy)alkane adducts of phosphine oxides superior oxidizing agents. Importantly, the phosphine oxide carrier is not reactive and non-toxic.

Selected other forms of peroxides that have been applied recently include urea hydrogen peroxide adducts,[19–21] organic peroxocarbonates,[22–24] peroxoborates [24] and organic peroxides.[25] For example, peroxoborates have been explored in diverse fields ranging

* Corresponding author.
E-mail address: bluemel@tamu.edu (J. Blümel).

https://doi.org/10.1016/j.apsusc.2023.157333
Received 17 March 2023; Received in revised form 17 April 2023; Accepted 19 April 2023
Available online 24 April 2023

from oral healthcare [26] to chemical warfare agent degradation,[27] while peroxocarbonates, phosphates and sulfates have been used as electrochemical waste-water disinfectants [28].

The remaining disadvantage of all di(hydroperoxy)alkane adducts compared to aqueous H_2O_2 is that the phosphine oxide carrier has to be removed from the product mixture after the reaction. The separation can easily be accomplished by precipitation with nonpolar organic solvents.[11] Nevertheless, this process represents one more required step following the oxidation reaction. Therefore, in this contribution, we describe a method that allows oxidation reactions to take place in one organic phase, while the surface-tethered phosphine oxide carrier can be removed by settling of the support within minutes. In this way, the phosphine oxide can be recharged with peroxide and the oxidizing agent can be reused multiple times. Most importantly, the targeted immobilized peroxides are all exposed to the substrates on the silica surface and in this way ensure efficient, homogeneous reactions. In contrast, solid inorganic peroxides like peroxocarbonates suffer from low solubility in organic solvents.

Some bifunctional phosphines incorporating ethoxysilane functionalities for immobilization on silica are available commercially. Alternatively, phosphines such as $Ph_2P(CH_2)_3Si(OEt)_3$ can easily be synthesized from $LiPPh_2$ and $Cl(CH_2)_3Si(OEt)_3$.[29,30] These phosphines can be covalently bound to the silica support according to well-established methods [29–35] or using a recently developed adsorption/dry heating process to avoid cross-linking of the ethoxysilanes and off-surface growth.[36] The formed Si-O-Si bonds to the surface are extremely robust and prevent leaching of the ligand once at least one covalent bond is established.[30] The large surface area of silica also allows for a high loading of the ligand onto the support.[30] The covalently surface-bound phosphine ligands can be oxidized to the phosphine oxides by treatment with aqueous hydrogen peroxide.[37]

Immobilizing the phosphine oxide carrier allows for the spent oxidizer that consists mainly of the phosphine oxide and its water adduct,[8,11,12] to be separated from the reaction mixture by settling. The di-(hydroperoxy)propane adduct can then be regenerated by adding H_2O_2 and acetone,[13–18] and reused. The desired product of the oxidation reaction is also recovered without need for further purification, rendering the adducts an even more attractive option for oxidations in academia and industry.

Importantly, previous work has shown that silica functionalized with ligands capable of hydrogen bonding to H_2O_2 could, in principle, offer greater peroxide loading than silica alone.[38] However, attempts at functionalizing silica were complicated by decomposition of the ligands when applying even dilute H_2O_2, which significantly lowered H_2O_2 capacity.[38] Additionally, the exact structures that the surface species assumed were not well defined.

Our contribution represents a substantial improvement, as immobilized ethoxysilanes and phosphine oxides are extremely robust under harsh reaction conditions.[30,37] In particular, the immobilized phosphine oxide carrier is not affected by applying H_2O_2.[37] Additionally, ^{31}P solid-state NMR allows for a convenient method of characterizing the stabilized peroxides on the surface. Characteristic differences in the ^{31}P chemical shift, residual halfwidth and chemical shift anisotropy (CSA, span of the signal) for neat phosphine oxides compared to adducts of phosphine oxides can be exploited.[39–44]

When adsorbing and covalently binding a bifunctional phosphine ligand onto silica,[36] there is the potential for phosphine oxide-surface interactions. Adsorbed triphenylphosphine oxide and alkylphosphine oxides, for example, have previously been shown to interact strongly with silica surfaces via the P=O group.[39–41,45–49] Phosphine oxides can also form adducts with $AlCl_3$ which is a Lewis acid, like some silica sites.[50] The ability of phosphine oxides to interact with the silica surface after they have been tethered to silica via Si-O-Si linkages has also been demonstrated. In these studies, it was found that lower surface coverages lead to a greater degree of surface interaction due to the favored blanket-type structure as opposed to a brush-type structure.[36] These interactions have the potential to play a large role in future applications of these materials as they may significantly impact the reactivity of the phosphine oxide. Therefore, the P=O-silica interactions will also be explored in the following research description.

This contribution presents the synthesis, characterization, regeneration, and reuse of a silica-immobilized Ahn adduct. The residual surface sites have been end-capped by reaction of the material with $EtOSi(CH_3)_3$.[31,33] ^{31}P MAS (magic angle spinning) NMR [42–44] of end-capped versus non-end-capped material is used to show that end-capping can prevent previously observed interactions of the phosphine oxide with the silica surface. The subsequently generated di(hydroperoxy)propane adduct of the immobilized phosphine oxide is then characterized via multinuclear solid-state NMR. The synthesis of an analogous deuterated molecular and silica-bound di(hydroperoxy)propane-d_6 adduct of a phosphine oxide is also presented. This deuterated version offers additional proof for the formation of di(hydroperoxy) propane adducts on silica while also allowing for insight into the strength of the adduct-phosphine oxide interactions. These interactions are further explored and the adduct moiety is characterized in solution through adduct washing experiments. Finally, the activity and recyclability of the new adduct material is confirmed via the oxidation of PPh_3 to $O{=}PPh_3$ [11,13,51,52] and the direct esterification of aldehydes [18,53–58].

In summary, the following outline presents a new route to easily accessible, well-defined surface-bound di(hydroperoxy)alkane adducts of phosphine oxides. These stable peroxides can easily be removed from the reaction mixtures by settling and regenerated for multiple cycles of reuse. The efficient oxidation of a phosphine to the phosphine oxide and the direct oxidative esterification of aldehydes [18] serve as reactions to prove the success of the novel oxidizer.

2. Results and discussion

2.1. Immobilizing the phosphine oxide carrier

The synthetic strategy for generating silica-immobilized di(hydroperoxy)propane adducts of a phosphine oxide is displayed in Fig. 1. For clarity, the immobilized ethoxysilanes are depicted with only one Si-O-Si linkage, although ^{29}Si CP/MAS NMR indicates there is a mixture of silanes bound to the surface by one, two, and three Si-O-Si linkages (see below).[30,32,36]

A sub-monolayer amount of **1** has been immobilized on silica using standard literature procedures to produce material **2** (Fig. 1).[29–35] The immobilization has not been performed while strictly working

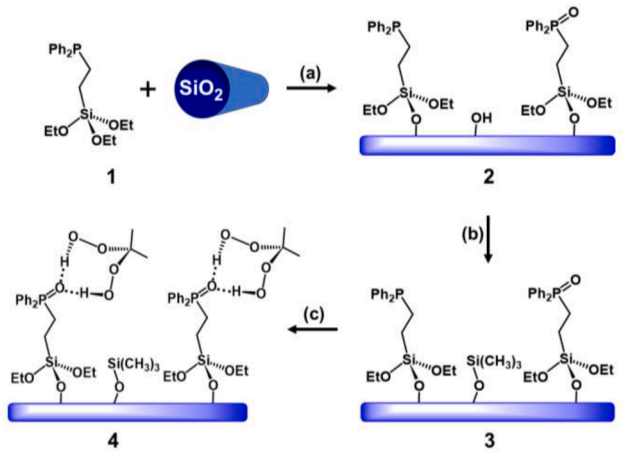

Fig. 1. Synthetic strategy for creating immobilized peroxide adducts starting from immobilization of **1**, followed by end-capping with ethoxytrimethylsilane and di(hydroperoxy)propane adduct formation. (a) Toluene, 42 h, 70 °C. (b) Me_3SiOEt in excess, 45 h, 70 °C. (c) Acetone, aqueous H_2O_2, 48 h, RT.

under inert gas conditions, because fully oxidized material is sought eventually. Therefore, a mixture of immobilized phosphine **1i** and its oxide **1i(O)** is obtained, as visible in the ^{31}P MAS spectrum of **2** (Fig. 2, top). The ^{29}Si CP/MAS spectrum (Figure S1) proves the covalent tethering of the ethoxysilyl groups to the silica support. The statistical mixture of one, two and three Si-O-Si linkages is in accordance with previous results for ethoxysilane immobilization using a dilute solution. [30–32,36]

The ^{13}C CP/MAS NMR spectrum of material **2** shows well-resolved signals even without employing DNP (Dynamic Nuclear Polarization) methods [59] that have been assigned completely (Figure S2). As expected from the ^{29}Si CP/MAS spectrum, there are ^{13}C signals for residual ethoxy groups at 61.06 (OCH_2) and 18.48 ppm (CH_3). Due to the residual mobility of phosphine linkers tethered via methylene chains, [30,33,60] even the alkyl and ethoxy proton signals are resolved in the ^{1}H MAS spectrum of **2** (Figure S3).

2.2. End-capping the surface with trimethylsilyl groups

The ultimate goal, as outlined in Fig. 1, is to create surface-bound di-(hydroperoxy)propane molecules that are stabilized by hydrogen-bonding to the phosphine oxide group. Unfortunately, surface silanol groups form hydrogen bonds with phosphine oxides, too. This has been explored previously for a variety of surface-adsorbed phosphine oxides. [38–41] Therefore, surface silanol groups are expected to compete with hydrogen-bonded peroxide for P=O groups. Given the large number of surface silanol groups, this competition could be detrimental for the planned immobilization of the peroxides and for creating material **4** (Fig. 1). In the specific case presented here, it can be demonstrated for the first time that the interactions of silanol groups with a covalently bound phosphine oxide takes place as well. While the $\delta(^{31}P)$ for **1i** at −8.95 ppm corresponds to the typical chemical shift of surface-bound alkyldiarylphosphine linkers,[30,36] the value of 41.99 ppm (Fig. 2, top) for the immobilized phosphine oxide **1i(O)** is comparatively high. [35,39–41] This indicates that hydrogen-bonding to silanol groups and therewith a deshielding of the phosphorus nucleus takes place. This deshielding upon surface adsorption has been observed previously for surface-adsorbed and molecular, hydrogen-bonded phosphine oxides. [6,11–18,39–41] Regarding the arrangement of the phosphine oxide molecules on the surface, one can imagine that in a sub-monolayer the covalently bound molecules are aligned parallel to the surface, in a blanket-type manner, as described for covalently bound phosphines recently.[36]

The competition for hydrogen-bonding that arises from surface silanol groups has to be eliminated prior to generating the desired peroxo adducts. Removing silanol protons can, in principle, be achieved by conventional end-capping with $ClSiMe_3$. However, this reaction creates HCl that is hard to remove from the surface, could potentially protonate **1i** and negatively impact the lifetime of the targeted immobilized peroxide. Therefore, an excess of the milder, but at elevated temperatures and longer reaction times equally efficient, end-capping reagent $EtOSi(CH_3)_3$ (EtOTMS) [31,33] has been added to **2** to produce the end-capped material **3** (Fig. 1). The successful co-immobilization of EtOTMS has been confirmed with ^{29}Si CP/MAS NMR (Figure S4). The spectrum prominently features the ^{29}Si signal of the TMS group with the expected chemical shift of 13.14 ppm in addition to the resonances of **1i**. Importantly, the halfwidth (325 Hz) of the signal speaks for covalent bonding to the surface, in contrast to merely adsorbed silane.[36]

The ^{13}C CP/MAS spectrum of **3** (Figure S5) shows the signal of the TMS group at 1.38 ppm in addition to the resonances of **1i**. Again, the large halfwidth of the signal (297 Hz) indicates that the TMS groups are covalently surface-bound.[36] Adsorbed EtOTMS would feature a sharp peak due to its higher mobility on the surface.[31,36] ^{1}H MAS NMR measurements corroborate the assumption that end-capped material **3** has been generated successfully (Figure S6).

The ^{31}P MAS spectrum of end-capped **3** in comparison with **2** completes the picture (Fig. 2, bottom). Since oxygen was not strictly excluded during the end-capping step, the signal of the phosphine oxide **1i(O)** grew at the expense of the resonance of **1i**. Since there are no longer any silanol groups on the silica surface that would withdraw electron density from phosphorus, the signal of **1i(O)** experiences an upfield shift from 41.99 ppm for **2** to 36.31 ppm for **3**. This difference in $\delta(^{31}P)$ of about 5 ppm has been consistently observed for a variety of other phosphine oxides and their electron withdrawing adducts. [6,11–18,39–41]

Besides liberating the P=O group of **1i(O)** from the surface and preparing it for the following peroxo adduct formation, end-capping the surface should also be beneficial with respect to repeated regeneration steps. The TMS groups render the surface of silica hydrophobic [31,61] and this effect, together with the steric shielding should help to protect the surface during the (re)generation of the immobilized di(hydroperoxy)propane **4** that requires aqueous H_2O_2. Furthermore, end-capping with EtOTMS prevents the products of oxidation reactions from strongly adsorbing at the silica surface, allowing for a clean separation from the silica by decanting, while extensive washing can be avoided. This is especially important for the oxidation products relevant in this contribution, $O = PPh_3$ and the methyl ester of nonanoic acid. It will also be demonstrated below that the surface-protecting TMS groups are retained over ten oxidation/regeneration cycles.

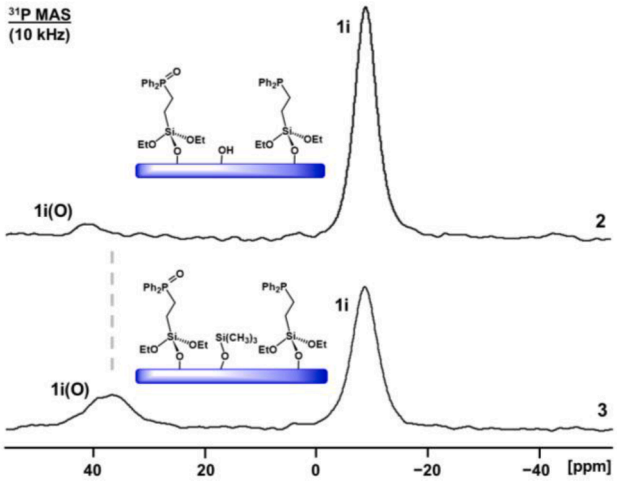

Fig. 2. ^{31}P MAS NMR spectra of starting material **2** and **3** after end-capping with EtOTMS.

2.3. Generating the immobilized peroxide

Next, the immobilized di(hydroperoxy)propane adduct **4** has been synthesized by stirring material **3** in a mixture of acetone and aqueous H_2O_2 at room temperature for two days.[13–18,37] After the reaction, the material was dried *in vacuo* and solid-state NMR has been used to characterize the sample. It should be noted that the adsorption of hydrogen peroxide on silica has previously been explored by theoretical calculations showing that H_2O_2 can form hydrogen bonding interactions on silica surfaces, particularly with Si-O-Si siloxane bridges.[63] However, siloxanes represent a small fraction of the available surface sites on silica relative to silanols, except after very harsh drying conditions. [31,64] Additionally, the adsorption of H_2O_2 is prevented by end-capping with EtOTMS.[31,62] It should also be noted that molecular di-(hydroperoxy)propane adducts are more shelf-stable than H_2O_2, [13–18] offering another advantage of the immobilized peroxides of **4** over simply adsorbing H_2O_2 on silica.[38]

When generating material **4** from **3**, a distinct change is obvious in the ^{31}P MAS NMR spectrum. The phosphine resonance vanished and one well-defined signal is obtained. The signal (Fig. 3) of **4** shifts downfield

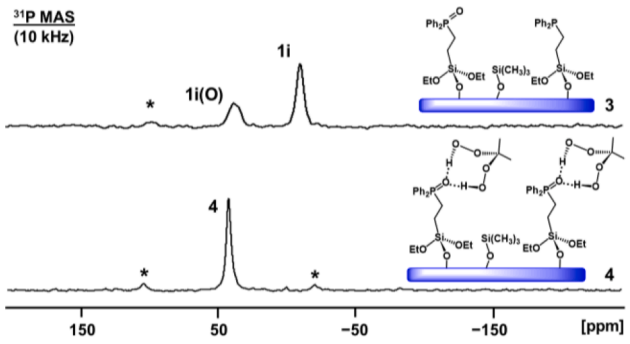

Fig. 3. ^{31}P MAS spectra of materials **3** and the immobilized di(hydroperoxy) propane **4**, obtained by treating **3** with aqueous H_2O_2 and acetone.

to 41.93 ppm compared to the signal of **1i(O)** in the spectrum of **3** at 39.51 ppm. Therefore, strong hydrogen-bonding of the P=O group to the di(hydroperoxy)propane group can be assumed, in accordance to the scenario of molecular adducts. Additionally, the halfwidth of the resonance decreases from 1.60 kHz for **1i(O)** in **3** to 0.98 kHz for **4**, which indicates that the P=O groups are experiencing a more homogeneous, well-defined surroundings than in material **3**.

^{29}Si and ^{13}C CP/MAS, as well as ^{1}H MAS NMR spectra of **4** (Figures S7, S8, S9) confirm that the material is well-defined, and all signals are accounted for. Importantly, the TMS groups remain intact after adduct formation. This eliminates the possibility that the downfield shift observed for **4** is caused by the phosphine oxide interacting with the silica surface as observed for **2** (Fig. 2). Interestingly, an increase in the signal intensities of the more upfield shifted Si-O-Si resonances in the range from −53 to −65 ppm indicates that the treatment of **3** with aqueous H_2O_2 and acetone increases the number of Si-O-Si linkages between the immobilized linkers and the silica surface (Figure S7). [36,65] This observation is consistent with results that show that applying aqueous H_2O_2 to ethoxysilanes induces cross-linking due to the presence of water and acid stabilizers in commercial H_2O_2 which catalyze this reaction [65].

2.4. Selectively deuterated immobilized peroxide

While the ^{31}P, ^{29}Si, ^{13}C, and ^{1}H solid-state NMR spectra clearly indicate the presence of the immobilized peroxide, the ^{1}H spectrum in particular suffers from intrinsic large dipolar interactions and a massive background signal of the silica support (Figure S9). Therefore, in order to unequivocally prove the presence of the di(hydroperoxy)propane moiety in **4**, the deuterated version **5** has been synthesized from **3** using acetone-d_6 (Fig. 4). In this way, CD_3 groups are incorporated into the adduct and **5** and its properties can be investigated with ^{2}H NMR using a solid-echo pulse program (Fig. 4 and Figure S10). Only one resonance with the chemical shift of 2.11 ppm, which is characteristic for $(CO)CD_3$ groups, is found in the ^{2}H NMR spectrum of **5**. No other ^{2}H signals are visible, which demonstrates that the deuterated immobilized peroxide adduct has been formed cleanly.

In order to prove that the ^{2}H NMR signal of **5** (Fig. 4) does not simply

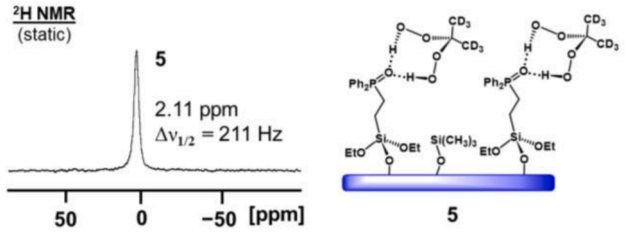

Fig. 4. Solid-echo ^{2}H NMR spectrum of a static sample of **5**, obtained from **3** by reaction with H_2O_2 and acetone-d_6.

stem from adsorbed deuterated acetone, the following experiments were performed. Acetone-d_6 vapor has been added to two rotors containing **3** and dried silica. Spectra of both materials were then recorded using the same measurement parameters as applied for the sample of **5**. All obtained ^{2}H NMR spectra are displayed in Figure S10. The resonance of **5** differs from the signals obtained for adsorbed acetone-d_6 regarding linewidths and chemical shifts. The signal of **5** is found upfield (2.11 ppm) compared to the signals of the adsorbed species (2.44 and 2.50 ppm), consistent with the reported ^{1}H NMR data for di(hydroperoxy) propane adducts in solution.[13–18] Furthermore, all ^{2}H NMR signals have different linewidths, indicating different degrees of mobility on the surface. Adsorbed acetone-d_6 on silica is most mobile and consequently displays the smallest signal halfwidth (128 Hz). This observation is in accordance with cases of other mobile species adsorbed on silica such as phosphine oxides and metallocenes [39–41,66–68]. Interestingly, the least mobile species with the largest signal halfwidth (334 Hz) is acetone-d_6 adsorbed on **3**. This indicates that **1**, **1i(O)** and TMS groups limit the mobility of acetone-d_6 on the surface. Even the CD_3 groups in the di (hydroperoxy)propane moiety of **5**, which is covalently bound to the silica via the phosphine oxide linker, are more mobile with a signal halfwidth of 211 Hz.

To further prove the presence of the deuterated di(hydroperoxy)-propane moiety in **5**, the two control samples and **5** were washed with non-deuterated acetone and dried in air. Then, all materials were investigated with ^{2}H solid-state NMR without rotation using the same measurement parameters (Figure S10). The ^{2}H signals of the two samples with adsorbed acetone-d_6 are completely removed while the resonance of **5** persists. Therefore, it can be concluded that the observed ^{2}H NMR signal (Fig. 4) belongs to the deuterated di(hydroperoxy)propane moiety. It persists throughout the intense washing step due to the strength of the hydrogen bonding between the peroxo moiety and the covalently bound phosphine oxide linker in **5**.

2.5. Studying the stability of the peroxide adducts

In order to assess the stability of the immobilized peroxide **4**, several key experiments have been performed. It has been shown by dynamic NMR earlier that different di(hydroperoxy)alkane moieties can exchange their phosphine oxide carriers in solution.[14] However, the question of whether or not a ketone can be oxidized and replace a di-(hydroperoxy)alkane moiety from a given phosphine oxide adduct still needs to be answered. For this purpose, the deuterated molecular adduct $Ph_3PO{\cdot}(HOO)_2C(CD_3)_2$ (**6**) has been synthesized according to the literature procedure.[13] This adduct is highly soluble and has been characterized by ^{31}P (Figure S11), ^{13}C (Figure S12), and ^{1}H NMR (Figure S13). All signals have been assigned based on the values of the non-deuterated version.[13] In particular, the septet of the CD_3 group in the ^{13}C NMR, and the lack of methyl proton signals in the ^{1}H NMR spectrum confirm that the di(hydroperoxy)propane moiety in adduct **6** is fully deuterated and intact. Furthermore, the dry powder of **6** displays the characteristic Pake pattern in the ^{2}H solid-state NMR spectrum (Figure S14). The key IR peaks of adduct **6** are in accordance with literature values, and show characteristic C-D stretching frequencies (Figure S15).

Next, **6** has been dissolved and stirred in an excess of non-deuterated acetone to determine whether exchange of the di(hydroperoxy)alkane moiety takes place or whether acetone can just remove the peroxo group from the immobilized adduct **5**. After the solvent was removed *in vacuo* the powder was measured with ^{31}P (Figure S11), ^{13}C (Figure S16), ^{1}H (Figure S17), and ^{2}H solid-state NMR (Figure S18). All spectra indicate that **6** is still the predominant species. This persistence of **6** also corroborates the washing results for **5** (Figure S10), which showed that the peroxo moiety is stable in the absence of an easily oxidizable substrate.

The ^{31}P NMR spectrum shows two minor decomposition products, the water adduct $(Ph_3P{=}O{\cdot}H_2O)_2$ (33.69 ppm) [11,12] and the oxide $Ph_3P{=}O$ (31.52 ppm) (Figure S11).[11] The fate of the deuterated di-

(hydroperoxy)propane has been monitored by probing the non-deuterated acetone that had been removed *in vacuo* with ^{2}H NMR (Figure S19). A signal corresponding to the CD_3 groups of acetone-d_6, stemming from the decomposition of the deuterated di(hydroperoxy)-propane moiety, was observed. This result explains why, despite the persistence of the CD_3 signal of **5**, its signal-to-noise ratio is diminished after the intensive acetone washing (Figure S10).

It has been demonstrated earlier using competition experiments that di(hydroperoxy)alkanes can be exchanged between different hydrogen-bonded phosphine oxides.[14] Therefore, it has been tested whether the di(hydroperoxy)propane moiety can be removed from **4** by another, strongly hydrogen-bonding species like water. In this way, indirect proof of the presence of the peroxo moiety in **4** can also be obtained.

In order to maximize the amount of di(hydroperoxy)propane moiety, a sample of **4** with a dense monolayer of linker was synthesized. The material was stirred in D_2O for one hour, then the supernatant was decanted and investigated by solution ^{1}H NMR spectroscopy. The first measurement was performed immediately, the second after 3 days (Fig. 5). Two resonances appear besides the large HOD peak at 4.6 ppm. They can be assigned to acetone (2.15 ppm) and the methyl protons of free di(hydroperoxy)propane **7** (1.35 ppm) [14]. The latter confirms that the di(hydroperoxy)propane moiety in **4** is accessible to D_2O and can be transferred into the aqueous solution. Since the signal intensity of **7** in solution is low, both samples were also compared to a control spectrum of the pristine solvent D_2O. Neither of the assigned peaks appear in this spectrum, and therefore, solvent impurities [69] can be excluded (Figure S20).

After 3 days, the di(hydroperoxy)propane peak decreased while the acetone peak increased correspondingly in intensity. This means that the liberated dihydroperoxide **7** decomposes gradually, forming acetone (Fig. 5) because in solution the peroxide is no longer stabilized by strong hydrogen-bonding to the phosphine oxide carrier. Furthermore, finding **7** in the D_2O solution affords further evidence that the immobilized di(hydroperoxy)propane adduct had successfully been generated in **4** and also shows that the di(hydroperoxy)propane remains stable for several days even in solution at room temperature.

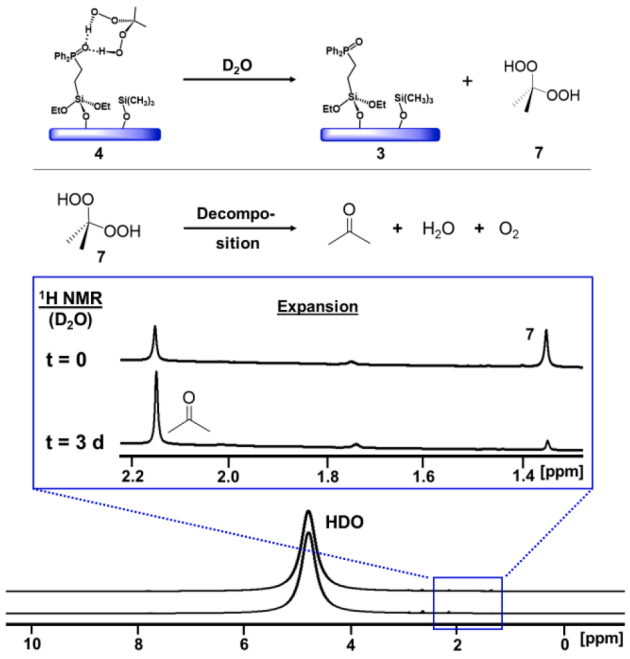

Fig. 5. When **4** is treated with D_2O, di(hydroperoxy)propane (**7**) is liberated and slowly decomposes in solution to yield acetone. ^{1}H NMR spectra of the supernatant were recorded immediately (top) and after 3 days (bottom).

2.6. Oxidation of PPh_3 to $O{=}PPh_3$ and regeneration of oxidizer

The immobilized peroxide **4** has been created to enable the easy removal of the phosphine oxide carrier from the reaction mixture and its recycling. Furthermore, the regeneration of the oxidizer on the surface was sought. In order to test these capabilities of the immobilized oxidizer, in a first step, the oxidation of PPh_3 to $O{=}PPh_3$ was monitored (Fig. 6). This reaction is a favorable choice because PPh_3 is practically not oxidized by oxygen in the air or dissolved oxygen [11,13,51]. In a control experiment, no oxidation was observed when PPh_3 was stirred in THF or with end-capped silica suspended in THF. As communicated earlier,[17] the di(hydroperoxy)alkane adducts perform the oxidation in a consecutive process, providing active oxygen atoms from both dihydroperoxy groups of one adduct assembly in a stepwise manner.

In a representative oxidation reaction, about two equivalents of PPh_3 were dissolved in THF, added to a flask containing **4** and the reaction mixtures was stirred for 30 min (Fig. 6). After the reaction and settling of the immobilized phosphine oxide carrier **3**, the supernatant was decanted. The silica support has been washed thoroughly to remove any $O{=}PPh_3$ or PPh_3 that might have remained adsorbed on the surface. [11,39–41] The supernatant and washing fractions were combined and analyzed by ^{31}P NMR. The ratio of substrate PPh_3 to product $O{=}PPh_3$ was then determined by integration and used to calculate the yield of the oxidation reaction, i.e. the amount of PPh_3 converted to $O{=}PPh_3$. This value corresponds to the amount of active oxygen that was present in **4**. The yield of oxidized substrate was then determined based upon the amount of **1** immobilized on the sample of **4**, assuming that there are two reactive oxygens per mole of **1**. After the reaction, **4** was regenerated by addition of acetone/H_2O_2 and the recyclability of **3** and successful regeneration of **4** was tested by repeating the procedure outlined in Fig. 6. The results of 10 cycles are summarized in Table 1.

The results in Table 1 show clearly that the phosphine oxide carrier **3** can be recycled and material **4** regenerated to oxidize substrates over multiple cycles. The decreasing activity seen after cycle 4 was probably a result of the silica pores being clogged with residual solvent from the washing procedures, which hindered diffusion of the dissolved substrate to the oxidizer on the surface. ^{1}H solid-state NMR of the material after cycle 6 further corroborated this assumption as large THF signals were observed (Figure S21). In order to remove the THF, the material was dried for 2 h *in vacuo* at 30 °C. The dried material showed decreased signal intensities for the THF peaks relative to the TMS signal (Figure S21). Furthermore, the yield improved after drying. The drying step was also applied between cycles 9 and 10, however, no further gain in yield was achieved. This suggests that progressively more intensive

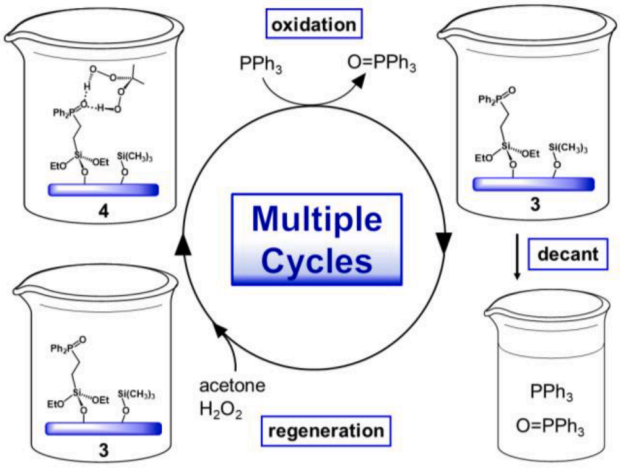

Fig. 6. Oxidation of PPh_3 to $O{=}PPh_3$ by **4**, removal of the phosphine oxide carrier by settling, decanting the supernatant containing the product and regenerating the oxidizer **4**.

Table 1
Repeated oxidation of PPh_3 to O=PPh_3 using one sample of **4**. The oxidizer is regenerated after each cycle with acetone/H_2O_2. In between cycles 6/7 and 9/10 the material was dried (2 h *in vacuo*, 30 °C). The asterisk denotes a cycle where **4** was stored for 5 days after regeneration before washing; the yield > 100% was due to residual H_2O_2 adsorbed on the surface.

Cycle	Yield of O=PPh_3 (%)
1	81
2	70
3*	106*
4	81
5	38
6	52
7	82
8	67
9	68
10	51

drying treatments may be needed in case more cycles are desired. Leaching of the phosphine oxide carrier **1i(O)** from the silica support can be ruled out. No NMR signal for **1(O)** (~34 ppm) or any other phosphine species besides PPh_3 and O=PPh_3 has been observed when the supernatant was measured after any of the 10 cycles. The spectrum from cycle 1 is shown as an example (Figure S22).

It should also be noted that the TMS surface-protecting groups are fully retained under the conditions used for both the oxidation of PPh_3 and the direct oxidative esterification described below. This can be seen in Figure S21, where the ^{1}H MAS signal of the TMS group persists over ten oxidation/regeneration cycles. When stored under the atmosphere for two months, some water is taken up from the atmosphere, however, the TMS groups are fully retained. Figure S7 provides corresponding ^{29}Si CP/MAS information. When **3** is treated with an aqueous acetone/H_2O_2 mixture, the TMS groups with a signal at about 15 ppm persist.

At this point it should be noted that surface-adsorbed H_2O_2 has the potential to play a role in the oxidation reaction. Previous work has shown the ability of H_2O_2 to adsorb on neat and functionalized silica. [38,63] In cycle 3, material **4** has been stored after regeneration for 5 days before being washed with water while for all other cycles **4** was washed immediately. This washing delay led to adsorbed H_2O_2 which was likely responsible for the over-oxidation observed in this cycle (Table 1). Despite the ability for excess H_2O_2 to adsorb onto **3** during adduct formation, the adducts are preferred as the phosphine oxide-stabilized di(hydroperoxy)propane moiety is more stable than H_2O_2 [17] and the formation of the adduct is dependent on the total amount of H_2O_2 applied, not on the concentration as is the case for adsorbed-only materials [38,63].

To prove that adsorbed H_2O_2 was not responsible for oxidation observed in the other cycles, **4** was studied by ^{31}P MAS NMR before and after the reaction with PPh_3 in cycle 1 (Fig. 7). After the oxidation there is a clear upfield shift of the isotropic line, from 42.97 ppm for **4** to 36.17 ppm for **3**. Additionally, the intensities of the rotational sidebands and therewith the CSA [42] of the signal increase when **4** is spent and **3** is generated. Furthermore, the residual linewidth changes from 0.7 kHz to 1.5 kHz. These results prove unequivocally that the immobilized di(hydroperoxy)propane **4**, and not adsorbed H_2O_2, is responsible for the oxidation of PPh_3. The ^{31}P MAS spectra displayed in Fig. 7 also demonstrate that no PPh_3 (~-5 ppm) or O=PPh_3 (~25 ppm) stay adsorbed on the silica surface after the oxidation. The spectra again confirm that the phosphine oxide linker **1i(O)** remains covalently bound to the surface.

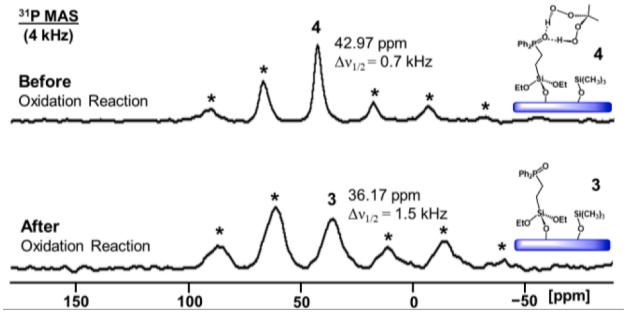

Fig. 7. ^{31}P MAS NMR spectra of material **4** before (top) and after the oxidation of PPh_3 (bottom).

2.7. Direct oxidative esterification of nonanal

In order to demonstrate that the immobilized peroxide **4** has merit for real-life syntheses in academia and industry, it was applied to the direct esterification of an aldehyde.[18] Molecular versions of di(hydroperoxy)alkane adducts of phosphine oxides have successfully been applied to the esterification of diverse aldehydes previously.[18] Hereby, $AlCl_3$ functions as an inexpensive, non-toxic Lewis acid catalyst. The only drawback of molecular adducts is that the phosphine oxide carrier interferes with the analytics in solution and has to be separated from the reaction mixture after the oxidation.[18] Using the process described above (Fig. 6), the immobilized phosphine oxide **3** can be removed by settling and recycled. The surface-bound peroxide **4** is re-generated with acetone/H_2O_2. Nonanal and methanol have been chosen as substrates, in combination with $AlCl_3$ as the catalyst (Fig. 8).

As an additional bonus of **4**, the water molecule generated by reducing the di(hydroperoxy)propane moiety will remain hydrogen-bonded to the immobilized phosphine oxide carrier.[6,11,12] In this way, the hydrolysis of the produced ester and of the catalyst $AlCl_3$ is avoided. This principle has been demonstrated recently for another moisture-sensitive reaction, the Baeyer-Villiger oxidation.[17] In order to minimize additional water uptake during the synthesis of **4**, it was washed with dry and degassed acetone and all esterification reactions have been performed under nitrogen.

The reaction success has been assessed by decanting the supernatant, removing the solvent *in vacuo* and analyzing the resulting oil by ^{1}H NMR spectroscopy (Figure S23). The α methylene protons vicinal to the carbonyl group have distinct and characteristic chemical shifts for the nonyl aldehyde, nonanoic acid and the methyl ester, respectively.[18] The ester formation has also been confirmed by the presence of a signal corresponding to the OCH_3 group at 3.65 ppm (Figure S23).

The results of three preliminary esterification experiments are summarized in Table 2. The first reaction **E1** led to a mixture of nonanoic acid and its methyl ester. The presence of the acid indicates that some water still remained on the silica despite washing it with dry acetone. The adduct was then regenerated and the reaction repeated (**E2**). But this time a small amount (200 mg) of dried silica was added along with the esterification reagents to sequester residual water on the

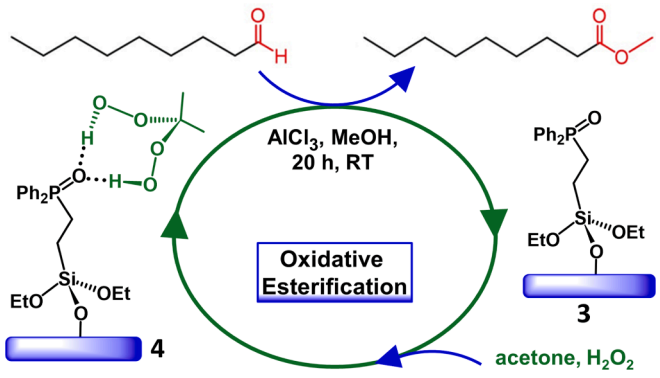

Fig. 8. Oxidative esterification of nonanal and regeneration of **4**.

Table 2
Results of three preliminary experiments **E1**-**E3** for the esterification of nonanal to the methyl ester of nonanoic acid using **4** as the oxygen source. Equivalents are based on the amount of active oxygen present in the sample of **4**, assuming that each immobilized phosphine oxide linker molecule contains two reactive oxygen atoms.

Experiment	E1	E2	E3
added dried silica (mg)	0	200	300
nonanal (eq)	0.71	0.77	0.97
methanol (eq)	55	150	376
$AlCl_3$ (eq)	0.51	0.96	0.96
aldehyde in product mixture (%)	62	25	28
acid in product mixture (%)	18	0	0
ester in product mixture (%)	20	75	72
yield (acid + ester) (%)	13	30	36

hygroscopic silica surface. This approach led to the acid-free formation of the ester in a respectable yield (30%). The reaction was repeated (**E3**), adding a larger amount of dried silica, and a slightly higher yield of 36% of ester has been obtained without acid byproduct. The results also prove that the catalyst $AlCl_3$ reaches the peroxide and substrate within the pores of **4**.

It should be noted that in all three experiments **E1**-**E3** (Table 2) the supernatant was checked by ^{31}P NMR and no signals were observed. This proves again that the phosphine oxide linker is not leaching during the reaction and remains on the silica. This eliminates the need to purify the reaction product and allows the di(hydroperoxy)propane adduct **4** to be regenerated. The less than quantitative yield may be due to the loss of some adduct from the silica during the acetone wash as this solvent has previously been shown to remove some of the peroxide from its phosphine oxide carrier (Fig. 5). Nevertheless, the data show that even under not optimized reaction conditions the principle of the immobilized peroxide works and ester is obtained under mild conditions.

3. Conclusion

In this contribution, we synthesized a new immobilized phosphine oxide **3**, and end-capped the silica surface with EtOTMS. By studying the functionalized material before and after end-capping with multinuclear solid-state NMR spectroscopy it has been demonstrated that the TMS groups prevent interactions between the phosphine oxide and the silica surface that may inhibit the subsequent adduct formation. After reaction with acetone/H_2O_2, the silica-bound di(hydroperoxy)propane adduct **4** has been obtained.

^{31}P MAS solid-state NMR was used to directly characterize the new adduct and observe the expected changes in the peroxide adduct compared to the phosphine oxide signal, including the downfield shift, reduced CSA and signal halfwidth. Further characterization has been achieved by synthesizing a deuterated version of the adduct (**5**) and applying ^{2}H NMR to directly confirm the structure and presence of the phosphine oxide-stabilized di(hydroperoxy)propane moiety. Treatment of **5** with acetone allowed the characterization of the molecular di(hydroperoxy)propane **7** in solution and offered insight into the strength of the phosphine oxide-adduct hydrogen bonds. The stability of **7** in solution has been monitored by observing its decomposition with solution ^{1}H NMR spectra.

Finally, the oxidative activity of the surface-bound peroxide **4** has been assessed by monitoring the oxidation of PPh_3 to $O{=}PPh_3$. The phosphine oxide linker has been recycled and **4** has been regenerated over 10 cycles while the system maintained its oxidative activity. Mild heating under vacuum was also shown to restore the adduct activity to initial levels by removal of residual solvent from the silica pores. Measuring solid-state ^{31}P MAS NMR of the oxidizing material before and after use proved that the observed oxidation originated from the adduct **4**, and not surface-adsorbed H_2O_2, as the observed signal clearly indicates a shift from the adduct **4** to the oxide **3**. The NMR also showed no residual PPh_3 or $O{=}PPh_3$ left adsorbed on the surface after the reaction. Furthermore, investigating the supernatant showed that no phosphine oxide linker leaches from the silica surface. This result has also been confirmed when **4** was regenerated and applied repeatedly as the active oxygen source for the direct esterification of nonanal to the nonanoic acid ester.

Overall, this contribution presents a new type of oxidizing material. The peroxide moiety contains two active oxygen atoms per molecule and is stabilized by strong hydrogen-bonding to a phosphine oxide group. This phosphine oxide carrier is covalently bound to a silica support. Therefore, it can be easily removed after the reaction by settling and it can be recycled. The di(hydroperoxy)propane group can be regenerated by reaction with acetone/H_2O_2. In contrast to solid oxidizers described previously, the presented material operates in one homogeneous phase and all active oxygen atoms are accessible for the substrates and the catalyst needed for the oxidative esterification. The principle of this new, safe, and long-lived surface-bound oxidizer and its regeneration can easily be adapted to other oxidation reactions and therefore it should have a bright future and ample application in synthetic chemistry and oxidation reactions.

4. Experimental section

4.1. NMR measurements

The ^{31}P, ^{13}C, ^{2}H and ^{1}H NMR spectra were recorded at RT on a 500 MHz Varian NMR spectrometer. Neat Ph_2PCl ($\delta(^{31}P) = +81.92$ ppm) in a sealed capillary centered in a 5 mm NMR tube was used as reference for the ^{31}P chemical shifts of dissolved compounds. The ^{13}C, ^{2}H and ^{1}H chemical shifts were referenced with respect to the solvent signals. ^{31}P NMR spectra for the quantification of the reactive oxygen content were acquired with a Varian decoupled-NOE pulse program and a 3 s relaxation delay. The ^{31}P solid-state NMR spectra were measured with a 400 MHz Bruker Avance NMR instrument using high-power proton decoupling and MAS in combination with 4 mm ZrO_2 rotors. The ^{31}P MAS spectra were calibrated using $NH_4H_2PO_4$ as an external standard ($\delta(^{31}P) = +0.81$ ppm). The ^{13}C CP/MAS solid-state NMR spectra were measured on the same instrument using a RAMP sequence. The spectra were calibrated with glycine as the external chemical shift standard ($\delta(^{13}CO) = 176.5$ ppm). The ^{1}H MAS spectra were measured with a single pulse program and acetone as the external standard ($\delta(^{1}H) = +2.05$ ppm). ^{2}H solid-state NMR spectra were recorded using a solid-echo pulse program and were calibrated with the external standard acetone-d_6 ($\delta(^{2}H) = +2.05$ ppm).

4.2. Materials and general reaction conditions

Reactions involving **2**, **3** and **6** were carried out using standard Schlenk techniques and a purified nitrogen atmosphere. All other reactions were performed in air. Toluene and tetrahydrofuran were obtained oxygen-free from a solvent purification system and were dried with 4 Å molecular sieves. Reagents purchased from Sigma Aldrich, VWR, Acros, Gelest and BTC were used without further purification. Aqueous H_2O_2 (35%) was obtained from Acros Organics and used as received. The exact concentration (13.3 M) was determined by titration with $KMnO_4$. The phosphine $(EtO)_3Si(CH_2)_2PPh_2$ (**1**) was purchased and its purity was confirmed with solution $^{31}P\{^{1}H\}$, $^{13}C\{^{1}H\}$ and ^{1}H NMR spectroscopy. The silica gel was acquired from Silicycle with a 40 Å average pore size, 0.063 to 0.2 mm particle diameter, and 750 m^2/g specific surface area. Before the reactions, the silica was dried *in vacuo* for 72 h at 300 °C in a Büchi glass oven.

4.3. Syntheses

Synthesis of **2**. In a representative reaction, **1** (1.0597 g, 2.8257 mmol) was added to an oven-dried Schlenk flask and dissolved in

toluene (10 mL). In a separate flask, dried silica gel (14.9585 g) was suspended in toluene (30 mL). The solution of **1** was then added to the silica. The reaction mixture was heated to 70 °C and stirred for 42 h. Subsequently, the supernatant was decanted, and **2** was washed 3 times with THF (15 mL, 20 min. stirring). Material **2** was then dried *in vacuo* for 5 h at RT. To determine the surface coverage, the solvent was removed *in vacuo* from the collected supernatant solutions and the residual ligand **1** was weighed (0.1203 g) and the obtained value subtracted from the initial mass of **1**. The surface coverage (62.8 mg per g of silica) was then determined as 55%, based on the full monolayer coverage of 114 mg **1** per g of silica determined previously.[36].

Synthesis of **3**. $EtOSiMe_3$ (27.515 g, 0.23268 mol) was added to the sample of **2** generated as described above and the mixture was stirred at 70 °C for 45 h. Then, the excess of $EtOSiMe_3$ was removed *in vacuo*. After 2.5 h, material **3** was stirred with THF (30 mL) and after settling, the supernatant was decanted and material **3** was dried again *in vacuo* for 2 h at RT.

Synthesis of **4** and **5**. Material **3** (1.8212 g, 0.2888 mmol **1**) was placed into a round-bottom flask. Acetone (10 mL) and aqueous H_2O_2 (0.500 mL, 13.3 M) were added to a scintillation vial and stirred for 5 min. The solution was transferred into the flask containing **3**, and the vial was rinsed with acetone (5 mL) which was also added to the flask. The reaction mixture was stirred for 42 h at RT. Then, the material was allowed to settle for 5 min. before the supernatant was removed with a pipette and vacuum-filtered through a fritted funnel using a side-arm flask. Deionized water (15 mL) was then added to the flask and the mixture was stirred for 20 s. The supernatant was again removed and vacuum-filtered. The modified silica **4**, collected on the frit, was added back into the original flask. The material was then immediately used for PPh_3 oxidation experiments. The deuterated material **5** was synthesized in the same way as **4** by using acetone-d_6 instead of acetone.

Synthesis of **6**. PPh_3 (507.8 mg, 2.176 mmol) was added to a Schlenk flask and dissolved in acetone-d_6 (15 mL). The flask was then cooled to 0 °C and aqueous H_2O_2 (1.5 mL) was added dropwise under stirring. The mixture was allowed to slowly warm to RT and was stirred for 16 h. Then, 10 mL of solvent was removed *in vacuo*. The remaining solution was added to an extraction funnel and an aqueous-organic extraction was performed using DCM and deionized H_2O. The DCM layer was collected and the solvent was removed *in vacuo* to yield **6** as an opaque colorless oil (145.0 mg, 0.370 mmol, 17% yield after crystallization).

4.4. Washing procedures for deuterated adducts *5* and *6*

For washing material **5** with acetone, an amount of **5** that was sufficient to fill a 4 mm MAS rotor was fully immersed in acetone for 5 min. The material was then air-dried, filled into the rotor and immediately measured. For the control experiments, approximately the same amount of **3** and unmodified dried silica were placed into different solid-state NMR rotors. Acetone-d_6 was then adsorbed onto the control materials by using a pipette to collect acetone-d_6 vapor from the headspace of a flask containing acetone-d_6 and expelling the pipette contents into the rotors. The rotors were capped and the samples immediately investigated with ^2H NMR. After the measurements, the contents of the samples were transferred to different test tubes and the same washing procedure used for **5** was applied to the control samples before they were measured again. The molecular deuterated adduct **6** was washed by combining polycrystalline **6** (150 mg) with acetone (10 mL) and stirring the mixture for 4 h. Then the solvent was removed *in vacuo*. The solvent and the obtained solid were investigated by NMR spectroscopy.

4.5. Washing procedures for a monolayer of adduct *4*

The immobilized adduct with a monolayer of **1** was synthesized in the same way as **4**. For the washing experiment the material (100 mg) was combined with D_2O (5 mL) and stirred for 1 h. The silica was allowed to settle for 20 min and a portion of the supernatant was collected with a pipette and added to an NMR tube for measurement. To verify that the observed signals originated from the washed adduct and not from solvent impurities a sample of the neat solvent D_2O was measured using the same acquisition parameters.

4.6. Oxidation of PPh_3

The following procedure was repeated for all oxidation cycles, with slight variations in the amount of PPh_3 (1.8–2.2 equivalents), except where noted (Table 1, Cycle 3). PPh_3 (531.8 mg, 2.028 mmol) was weighed into a scintillation vial and dissolved in 8 mL of THF. The solution was added under stirring to a flask containing 2.4879 g of **4**. 5 mL of THF was used to rinse the scintillation vial and also added to the reaction mixture. After 30 min. of stirring the supernatant was removed with a pipette and vacuum filtered through a fritted funnel using a side-arm flask. Next, THF (15 mL) was added to the reaction flask and the suspension was stirred for 20 min. Then the supernatant was removed with a pipette and filtered as outlined before. This was repeated 2 more times for a total of 3 washing cycles. After the final washing cycle a portion of the supernatant was filled into an NMR tube for measurement. The residual silica material collected on the fritted funnel was returned into the reaction flask, the material was dried *in vacuo* for 15 min. and regenerated according to the procedure for the synthesis of **4** described above. In between the cycles 6/7 and 9/10, the material was dried for 2 h *in vacuo* at 30 °C.

4.7. Direct oxidative esterification of nonyl aldehyde

The immobilized oxidizer **4** was generated as described under *4.3.* above, except that water-free, degassed acetone was used and the reaction mixture was stirred under nitrogen. After stirring for 42 h, the supernatant was removed and filtered. Water-free and degassed acetone (10 mL) was added to the adduct under a nitrogen stream and the mixture was stirred for 2 min. The supernatant was removed under nitrogen and filtered. This was repeated two more times for a total of 3 washing cycles. $AlCl_3$, nonanal and methanol were added into a 150 mL oven-dried Schlenk flask under nitrogen. Then water-free, degassed DCM was added until the $AlCl_3$ was dissolved and a clear solution was obtained. This solution was then transferred to the flask containing **4**. The mixture was stirred under nitrogen for 20 h. The supernatant was then collected and filtered through a frit into a Schlenk flask. Water-free, degassed THF (10 mL) was added to the flask containing the spent oxidizer and the mixture was stirred for 5 min. The supernatant was removed and filtered into the Schlenk flask with the reaction mixture. The THF washing was repeated 2 more times for a total of 3 washes. The solvent was then removed from the collected washing solutions *in vacuo* to yield a colorless oil. A portion of the oil was then dissolved in $CDCl_3$ and ^1H and $^{31}P\{^1H\}$ NMR spectra were collected. The spent oxidizer was dried *in vacuo* at 50 °C, regenerated to **4** with aqueous H_2O_2/acetone as described above, and reused for subsequent oxidation cycles. The second and third esterification procedures followed the same protocol as the first, except that only 1 acetone washing step was performed after the adduct formation and that dried silica was added to **4** prior to adding the DCM solution with the esterification reagents.

Declaration of Competing Interest

The authors declare that they have no known competing financial interests or personal relationships that could have appeared to influence the work reported in this paper.

Data availability

Data will be made available on request.

Acknowledgments

This work was supported by the National Science Foundation (CHE-1900100). Arturo J. Perez was supported by the NSF REU grant CHE 1851936.

Appendix A. Supplementary material

Supplementary data to this article can be found online at https://doi.org/10.1016/j.apsusc.2023.157333.

References

[1] D. Duprey, F. Cavani, Handbook of Advanced Methods and Processes in Oxidation Catalysis, Imperial College Press, 2014.
[2] F. Cavani, J.H. Teles, Sustainability in catalytic oxidation: an alternative approach or a structural evolution? ChemSusChem 2 (2009) 508–534.
[3] A.E. Comyns, Peroxides and Peroxide Compounds, in Van Nostrand's Encyclopedia of Chemistry, John Wiley & Sons, Inc., 2005.
[4] J. Maida, Hydrogen Peroxide Market to record USD 461.92 Mn growth - Driven by increasing demand from pulp and paper industry, *Yahoo! Finance* 2022, https://finance.yahoo.com/news/hydrogen-peroxide-market-record-usd-151500327.html.
[5] N.V. Klassen, D. Marchington, H.C.E. McGowan, H_2O_2 Determination by the I_3 Method and by $KMnO_4$ Titration", Anal. Chem. 66 (1994) 2921-2925.
[6] S. Kharel, N. Bhuvanesh, J.A. Gladysz, J. Blümel, New hydrogen bonding motifs of phosphine oxides with a silanediol, a phenol, and chloroform, Inorg. Chim. Acta 490 (2019) 215-219.
[7] E.Y. Tupikina, M. Bodensteiner, P.M. Tolstoy, G.S. Denisov, I.G. Shenderovich, P═O Moiety as an ambidextrous hydrogen bond acceptor, J. Phys. Chem. C 2018, 122, 1711-1720.
[8] G. Begimova, E.Y. Tupikina, V.K. Yu, G.S. Denisov, M. Bodensteiner, I.G. Shenderovich, Effect of hydrogen bonding to water on the ^{31}p chemical shift tensor of phenyl- and trialkylphosphine oxides and α-amino phosphonates, J. Phys. Chem. C 2016, 120, 8717-8729.
[9] R. Cuypers, E.J.R. Sudhölter, H. Zuilhof, Hydrogen bonding in phosphine oxide/phosphate–phenol complexes, ChemPhysChem 11 (2010) 2230–2240.
[10] N.A. Bewick, A. Arendt, Y. Li, S. Szafert, T. Lis, K.A. Wheeler, J. Young, R. Dembinski, Synthesis and solid-state structure of (4-hydroxy-3,5-diiodophenyl) phosphine oxides. Dimeric Motifs with the Assistance of O-H···O═P Hydrogen Bonds, Curr. Org. Chem. 19 (2015) 469-474.
[11] C.R. Hilliard, N. Bhuvanesh, J.A. Gladysz, J. Blümel, Synthesis, purification, and characterization of phosphine oxides and their hydrogen peroxide adducts, Dalton Trans. 41 (2012) 1742–1754.
[12] F.F. Arp, N. Bhuvanesh, J. Blümel, Hydrogen peroxide adducts of triarylphosphine oxides, Dalton Trans. 48 (2019) 14312-14325.
[13] S.H. Ahn, K.J. Cluff, N. Bhuvanesh, J. Blümel, Hydrogen peroxide and di (hydroperoxy)propane adducts of phosphine oxides as stoichiometric and soluble oxidizing agents, Angew. Chem. 2015, 127, 13539-13543. Angew. Chem. Int. Ed. 2015, 54, 13341-13345.
[14] F.F. Arp, N. Bhuvanesh, J. Blümel, Di(hydroperoxy)cycloalkane adducts of triarylphosphine oxides: a comprehensive study including solid-state structures and association in solution, Inorg. Chem. 59 (2020) 13719-13732.
[15] F.F. Arp, S.H. Ahn, N. Bhuvanesh, J. Blümel, Selective synthesis and stabilization of peroxides via phosphine oxides, New J. Chem. 43 (2019) 17174–17181.
[16] S.H. Ahn, N. Bhuvanesh, J. Blümel, Di(hydroperoxy)alkane adducts of phosphine oxides: safe, solid, stoichiometric, and soluble oxidizing agents, Chem. Eur. J. 23 (2017) 16998-17009.
[17] S.H. Ahn, D. Lindhardt, N. Bhuvanesh, J. Blümel,Di(hydroperoxy)cycloalkanes stabilized via hydrogen bonding by phosphine oxides: safe and efficient Baeyer-Villiger Oxidants, ACS Sustainable Chem. Eng. 6 (2018) 6829–6840.
[18] F.F. Arp, R. Ashirov, N. Bhuvanesh, J. Blümel, Di(hydroperoxy)adamantane adducts: synthesis, characterization and application as oxidizers for the direct esterification of aldehydes, Dalton Trans. 50 (2021) 15296-15309.
[19] M. Azizi, A. Maleki, F. Hakimpoor, Solvent, metal- and halogen-free synthesis of sulfoxides by using a recoverable heterogeneous urea-hydrogen peroxide silica-based oxidative catalytic system, Catal. Commun. 100 (2017) 62–65.
[20] S. Taliansky, Urea-Hydrogen peroxide complex, Synlett 12 (2005) 1962-1963.
[21] L. Ji, Y.-N. Wang, C. Qian, X.-Z. Chen, Nitrile-promoted alkene epoxidation with urea-hydrogen peroxide (UHP), Synthesis Commun. 43 (2013) 2256–2264.
[22] N. Koukabi, Sodium percarbonate: a versatile oxidizing reagent, Synlett 19 (2010) 2969-2970.
[23] A. McKillop, W.R. Sanderson, Sodium perborate and sodium percarbonate: further applications in organic synthesis, J. Chem. Soc., Perkin Trans. 1 (2000) 471–476.
[24] D. Habibi, M.A. Zolfigol, M. Safaiee, A. Shamsian, A. Ghorbani-Choghamarani, Catalytic oxidation of sulfides to sulfoxides using sodium perborate and/or sodium percarbonate and silica sulfuric acid in the presence of KBr, Catal. Commun. 10 (2009) 1257–1260.
[25] A.V. Arzumanyan, R.A. Novikov, A.O. Terent'ev, M.M. Platonov, V.G. Lakhtin, D.E. Arkhipov, A.A. Korlyukov, V.V. Chernyshev, A.N. Fitch, A.T. Zdvizhkov, I.B. Krylov, Y.V. Tomilov, G.I. Nikishin, Nature chooses rings: synthesis of silicon-containing macrocyclic peroxides, Organometallics 33 (2014) 2230-2246, and refs. cited.
[26] M. Grootveld, E. Lynch, G. Page, W. Chan, B. Percival, E. Anagnostaki, V. Mylona, S. Bordin-Aykroyd, K.L. Grootveld, Potential Advantages of Peroxoborates and Their Ester Adducts over Hydrogen Peroxide as Therapeutic Agents in Oral Healthcare Products: Chemical/Biochemical Reactivity Considerations in Vitro, Ex Vivo and in Vivo, Dent. J. 8 (2020) 89–132.
[27] S. Zhao, H. Xi, Y. Zuo, S. Han, Y. Zhu, Z. Li, L. Yuan, Z. Wang, C. Liu, Rapid Activation of Basic Hydrogen Peroxide by Borate and Efficient Destruction of Toxic Industrial Chemicals (TICs) and Chemical Warfare Agents (CWAs), J. Hazard. Mater. 367 (2019) 91–98.
[28] K.G. Serrano, A critical review on the electrochemical production and use of peroxo-compounds, Curr. Opin. Electrochem. 27 (2021) 1–7.
[29] K.D. Behringer, J. Blümel, Immobilization of carbonylnickel complexes: a solid-state NMR Study, Inorg. Chem. 35 (1996) 1814-1819.
[30] C. Merckle, J. Blümel, Bifunctional phosphines immobilized on inorganic oxides, Chem. Mater. 13 (2001) 3617–3623.
[31] J. Blümel, Reactions of ethoxysilanes with silica: a solid-state NMR study, J. Am. Chem. Soc. 1995, 117, 2112–2113.
[32] K.D. Behringer, J. Blümel, Reactions of ethoxysilanes with silica: a solid-state NMR study, J. Liq. Chrom. Rel. Technol. 19 (1996) 2753–2765.
[33] J. Guenther, J. Reibenspies, J. Blümel, Synthesis and characterization of tridentate phosphine ligands incorporating long methylene chains and ethoxysilane groups for immobilizing molecular rhodium catalysts, Mol. Catal. 479 (2019) 110629-110642.
[34] J.C. Pope, T. Posset, N. Bhuvanesh, J. Blümel, The palladium component of an immobilized Sonogashira catalyst system: new insights by multinuclear HRMAS NMR spectroscopy, Organometallics 33 (2014) 6750–6753.
[35] J. Blümel, Linkers and catalysts immobilized on oxide supports: new insights by solid-state NMR spectroscopy, Coord. Chem. Rev. 252 (2008) 2410-2423.
[36] E. Shakeri, J. Blümel, Creating well-defined monolayers of phosphine linkers incorporating ethoxysilyl groups on silica surfaces for superior immobilized catalysts, Appl. Surf. Sci. 615 (2023) 156380-156387.
[37] J. Blümel, Reactions of phosphines with silica: a solid-state NMR study, Inorg. Chem. 33 (1994) 5050-5056.
[38] D. Lewandowski, D. Bajerlein, G. Schroeder, Adsorption of hydrogen peroxide on functionalized mesoporous silica surfaces, Struct. Chem. 25 (2014) 1505–1512.
[39] P.J. Hubbard, J.W. Benzie, V.I. Bakhmutov, J. Blümel, Disentangling different modes of mobility of triphenylphosphine oxide adsorbed on alumina, J. Chem. Phys. 152 (2020) 054718-1-054718-8.
[40] S. Kharel, K.J. Cluff, N. Bhuvanesh, J.A. Gladysz, J. Blümel, Structures and Dynamics of Secondary and Tertiary Alkylphosphine Oxides Adsorbed on Silica, Chem. Asian J. 14 (2019) 2704-2711.
[41] C.R. Hilliard, S. Kharel, K.J. Cluff, N. Bhuvanesh, J.A. Gladysz, J. Blümel, Structures and unexpected dynamic properties of phosphine oxides adsorbed on silica surfaces, Chem. Eur. J. 20 (2014) 17292–17295.
[42] I.G. Shenderovich, H.-H. Limbach, Solid state NMR for nonexperts: an overview of simple but general practical methods, Solids 2 (2021) 139-154.
[43] J. Sommer, Y. Yang, D. Rambow, J. Blümel, Immobilization of phosphines on silica: identification of byproducts via ^{31}P CP/MAS Studies of Model Alkyl-, Aryl-, and Ethoxyphosphonium Salts, Inorg. Chem. 43 (2004) 7561-7563.
[44] I.G. Shenderovich, For Whom a puddle is the sea? Adsorption of organic guests on hydrated MCM-41 silica, Langmuir 36 (2020) 11383-11392.
[45] A. Zheng, S.-B. Liu, F. Deng, ^{31}P NMR chemical shifts of phosphorus probes as reliable and practical acidity scales for solid and liquid catalysts, Chem. Rev. 117 (2017) 12475–12531.
[46] R. Yerushalmi, J.C. Ho, Z. Fan, A. Javey, Phosphine oxide monolayers on SiO_2 surfaces, Angew. Chem. Int. Ed. 47 (2008) 4440-4442.
[47] J.P. Osegovic, R.S. Drago, Measurement of the Global Acidity of Solid Acids by ^{31}P MAS NMR of Chemisorbed Triethylphosphine Oxide, J. Phys. Chem. B, 2000, 104, 147-154.
[48] S. Hayashi, K. Jimura, N. Kojima, Adsorption of trimethylphosphine oxide on silicalite studied by solid-state NMR, Bull. Chem. Soc. Jpn. 87 (2014) 69–75.
[49] S. Machida, M. Sohmiya, Y. Ide, Y. Sugahara, Solid-state ^{31}P nuclear magnetic resonance study of interlayer hydroxide surfaces of kaolinite probed with an interlayer triethylphosphine oxide monolayer, Langmuir 34 (2018) 12694–12701.
[50] R. Ashirov, M. Kimball, M. O'Brien, N. Bhuvanesh, J. Blümel, Aluminum trichloride adducts of phosphine oxides: a single crystal X-Ray and Solid-State NMR Study, Inorg. Chem. (2023) in preparation.
[51] T.E. Barder, S.L. Buchwald, Rationale behind the resistance of dialkylbiaryl phosphines toward oxidation by molecular oxygen, J. Am. Chem. Soc. 129 (2007) 5096–5101.
[52] T. Tsuneda, J. Miyake, K. Miyatake, Mechanism of H_2O_2 decomposition by triphenylphosphine oxide, ACS Omega 3 (2018) 259–265.
[53] W. Harnying, P. Sudkaow, A. Biswas, A. Berkessel, N-heterocyclic carbene/carboxylic acid co-catalysis enables oxidative esterification of demanding aldehydes/enals, at low catalyst loading, Angew. Chem. Int. Ed. 2021, 60, 19631-19636.
[54] S. Gaspa, A. Porcheddu, L. De Luca, Recent developments in oxidative esterification and amidation of aldehydes, Tetrahedron Lett. 57 (2016) 3433–3440.
[55] C. Liu, L. Zheng, D. Liu, H. Zhang, A. Lei, Covalently bound benzyl ligand promotes selective palladium-catalyzed oxidative esterification of aldehydes with alcohols, Angew. Chem., Int. Ed. 51 (2012) 5662–5666.
[56] S.T. Goralski, K.M. Cid-Seara, J.J. Jarju, L. Rodriguez-Lorenzo, A.P. LaGrow, M. J. Rose, L.M. Salonen, Threefold reactivity of a COF-embedded rhenium catalyst: reductive etherification, oxidative esterification or transfer hydrogenation, Chem. Commun. 58 (2022) 12074–12077.

[57] J. Zhao, C. Much-Lichtenfeld, A. Studer, Cooperative N-heterocyclic carbene (NHC) and ruthenium redox catalysis: oxidative esterification of aldehydes with air as the terminal oxidant, Adv. Synth. Catal. 355 (2013) 1098–1106.
[58] K.K. Samudrala, W. Huynh, R.W. Dorn, A.J. Rossini, M.P. Conley, Formation of a strong heterogeneous aluminum Lewis acid on silica, Angew. Chem. Int. Ed. 2022, 61, e202205745-e202205750.
[59] S.L. Carnahan, Y. Chen, J.F. Wishart, J.W. Lubach, A.J. Rossini, Magic angle spinning dynamic nuclear polarization solid-state NMR spectroscopy of γ-irradiated molecular organic solids, Solid State Nucl. Magn. Reson. 119 (2022) 101785–101794.
[60] T. Posset, J. Guenther, J. Pope, T. Oeser, J. Blümel, Immobilized Sonogashira catalyst systems: new insights by multinuclear HRMAS NMR studies, Chem. Commun. 47 (2011) 2059–2061.
[61] R.P.W. Scott, Silica Gel and Bonded Phases, John Wiley and Sons: New York, 1993.
[62] J. Zegliński, G.P. Piotrowski, R. Piekoś, A study of interaction between hydrogen peroxide and silica gel by FTIR spectroscopy and quantum chemistry, J. Mol. Struct. 794 (2006) 83–91.
[63] L.T. Zhuralev, The surface chemistry of amorphous silica. Zhuravlev model, Colloids Surf. A Physicochem. Eng. Asp., 173 (2000) 1–38.
[64] S.A. Torry, A. Campbell, A.V. Cunliffe, D.A. Tod, Kinetic analysis of organosilane hydrolysis and condensation, Int. J. Adhes. 26 (2006) 40–49.
[65] K. Adachi, T. Hirano, The utility of sulfonic acid catalysts for silane water-crosslinked network formation in the ethylene-propylene copolymer system, J. Sol-Gel Sci. Technol. 49 (2009) 186–195.
[66] K.J. Cluff, J. Blümel, Adsorption of metallocenes on silica, Chem. Eur. J. 22 (2016) 16562–16575.
[67] P.J. Hubbard, J.W. Benzie, V.I. Bakhmutov, J. Blümel, Ferrocene adsorbed on silica and activated carbon surfaces: a solid-state NMR study of molecular dynamics and surface interactions, Organometallics 39 (2020) 1080–1091.
[68] J.W. Benzie, G.E. Harmon-Welch, J.C. Hoefler, V.I. Bakhmutov, J. Blümel, Molecular dynamics and surface interactions of nickelocene adsorbed on silica: a paramagnetic solid-state NMR study, Langmuir 38 (2022) 7422–7432.
[69] G.R. Fulmer, A.J.M. Miller, N.H. Sherden, H.E. Gottlieb, A. Nudelman, B.M. Stoltz, J.E. Bercaw, K.I. Goldberg, NMR chemical shifts of trace impurities: common laboratory solvents, organics, and gases in deuterated solvents relevant to the organometallic chemist, Organometallics 29 (2010) 2176–2179.